CD47 plays a critical role in T-cell recruitment by regulation of LFA-1 and VLA-4 integrin adhesive functions

Veronica Azcutia[a,b], Matthew Routledge[a,*], Marcie R. Williams[a,b], Gail Newton[a], William A. Frazier[c], Andrè Manica[d,e], Kevin J. Croce[b,e], Charles A. Parkos[f], Angela B. Schmider[b,g], Melissa V. Turman[b,g], Roy J. Soberman[b,g], and Francis W. Luscinskas[a,b]

[a]Center for Excellence in Vascular Biology, Department of Pathology, and [e]Cardiovascular Division, Department of Medicine, Brigham and Women's Hospital, Boston, MA 02115; [b]Harvard Medical School, Boston, MA 02115; [c]Department of Biochemistry and Molecular Biophysics, Washington University, St. Louis, MO 63130; [d]Instituto de Cardiologia do Rio Grande do Sul, Fundação Universitária de Cardiologia, Porto Alegre 90010-395, Brazil; [f]Division of Gastrointestinal Pathology, Emory University School of Medicine, Atlanta, GA 30322; [g]Division of Nephrology, Department of Medicine, Massachusetts General Hospital, Boston, MA 02114

ABSTRACT CD47 plays an important but incompletely understood role in the innate and adaptive immune responses. CD47, also called integrin-associated protein, has been demonstrated to associate in *cis* with $\beta 1$ and $\beta 3$ integrins. Here we test the hypothesis that CD47 regulates adhesive functions of T-cell $\alpha 4\beta 1$ (VLA-4) and $\alpha L\beta 2$ (LFA-1) in in vivo and in vitro models of inflammation. Intravital microscopy studies reveal that CD47$^{-/-}$ Th1 cells exhibit reduced interactions with wild-type (WT) inflamed cremaster muscle microvessels. Similarly, murine CD47$^{-/-}$ Th1 cells, as compared with WT, showed defects in adhesion and transmigration across tumor necrosis factor-α (TNF-α)–activated murine endothelium and in adhesion to immobilized intercellular adhesion molecule 1 (ICAM-1) and vascular cell adhesion protein 1 (VCAM-1) under flow conditions. Human Jurkat T-cells lacking CD47 also showed reduced adhesion to TNF-α–activated endothelium and ICAM-1 and VCAM-1. In *cis* interactions between Jurkat T-cell $\beta 2$ integrins and CD47 were detected by fluorescence lifetime imaging microscopy. Unexpectedly, Jurkat CD47 null cells exhibited a striking defect in $\beta 1$ and $\beta 2$ integrin activation in response to Mn^{2+} or Mg^{2+}/ethylene glycol tetraacetic acid treatment. Our results demonstrate that CD47 associates with $\beta 2$ integrins and is necessary to induce high-affinity conformations of LFA-1 and VLA-4 that recognize their endothelial cell ligands and support leukocyte adhesion and transendothelial migration.

INTRODUCTION

CD47 is a ubiquitously expressed 50-kDa transmembrane glycoprotein with a single immunoglobulin G (Ig)-like domain, a hydrophobic, five transmembrane-spanning segment, and a short hydrophobic cytoplasmic tail (Brown et al., 1990). CD47 has also been called integrin-associated protein because of its demonstrated ability to interact in *cis* with $\alpha v\beta 3$, $\alpha IIb\beta 3$, $\alpha 2\beta 1$, and $\alpha 4\beta 1$ integrins in nonleukocyte cell types (reviewed in Brown and Frazier, 2001). CD47 also interacts in *trans* with signal regulatory proteins (SIRPs) and thrombospondin (TSP; reviewed in Barclay, 2009). CD47 is involved in a broad range of important physiological processes, including leukocyte phagocytosis, recognition of "self," immune cell homeostasis, cell migration and regulation, leukocyte transendothelial and transepithelial

migration, platelet adhesion and activation, and nitric oxide signaling (Brown and Frazier, 2001; Isenberg et al., 2008).

Previous studies in CD47−/− mice established that CD47 plays a role in neutrophil emigration in a bacteria-induced peritonitis model (Lindberg et al., 1996), a lipopolysaccharide-induced, neutrophil-mediated acute lung injury and a bacterial pneumonia model (Su et al., 2008), and in vitro models of human neutrophil and monocyte transmigration across endothelium (Cooper et al., 1995; de Vries et al., 2002) and epithelium (Parkos et al., 1996). CD47 also was implicated in dendritic cell recruitment in a trinitrobenzenesulfonic acid–induced colitis model of hapten-stimulated inflammation (Fortin et al., 2009) and T-cell activation in the myelin oligodendrocyte glycoprotein–induced experimental autoimmune encephalomyelitis model (Han et al., 2012). We recently reported that human endothelial CD47 interacts with T-cell–expressed SIRPγ during T-cell transendothelial migration (TEM) under flow conditions in vitro (Stefanidakis et al., 2008). We also reported that CD47−/− mice showed reduced recruitment of blood T-cells, neutrophils, and monocytes in a dermal air pouch model of tumor necrosis factor-α (TNF-α)–induced inflammation and both endothelial- and leukocyte-expressed CD47s were required (Azcutia et al., 2012). On the basis of our findings that T-cells show significantly reduced recruitment in murine models in vivo and in human and murine in vitro models of inflammation, we investigated whether the defect is related to loss of CD47-dependent integrin adhesive functions.

The results of our study indicate that CD47 associates with T-cell β2 integrins as assessed by fluorescence lifetime imaging microscopy (FLIM) and CD47 is necessary for induction of VLA-4 and LFA-1 integrin high-affinity conformations that bind to their ligands vascular cell adhesion protein 1 (VCAM-1) and intercellular adhesion molecule 1 (ICAM-1), respectively. Our results suggest that in cis CD47–integrin associations, together with the previously reported in trans CD47–SIRP interactions (Stefanidakis et al., 2008), are important for both adhesion and transmigration across the vascular endothelium in in vivo and in vitro models of inflammation.

RESULTS

CD47−/− Th1 cells exhibit defective adhesive interactions with TNF-α–activated endothelium in the murine cremaster microvasculature

To evaluate the role of CD47 in leukocyte adhesive interactions with endothelium in vivo, we performed intravital microscopy studies in the murine cremaster microcirculation after intrascrotal injection of TNF as described earlier (Alcaide et al., 2012). Equal numbers of in vitro–generated wild-type (WT) and CD47−/− Th1 effector cells, each labeled with a different color fluorescent dye, were coinjected into WT recipient animals to enable comparison of WT and CD47−/− Th1 cells in the same postcapillary venules. The microvessel parameters for WT and CD47−/− mice are listed in Table 1. The behavior of transferred Th1 cells was monitored for 2–5 min postinjection. CD47−/− Th1 cells exhibited significantly reduced tethering adhesive interactions relative to WT Th1 cells (Figure 1A). The reciprocal experiment of simultaneous injection of differentially fluorescent-labeled WT and CD47−/− Th1 cells into CD47−/− recipient mice revealed that CD47−/− Th1 cells interacted less than did WT cells. Tethered Th1 cells become stably bound to the inflamed vessel wall for more than three consecutive video frames (~2 s). Few, if any, of the transferred T-cells arrest for more than several seconds. These results indicate expression of CD47 in T-cells is required for optimal Th1 effector cell adhesive interactions in this model. There was no difference between WT and CD47−/− T-cells in the rolling velocities, indicating that CD47 was not involved in Th1 cell rolling on inflamed venules (Figure 1B). This adhesion defect is not explained by reduced expression of adhesion molecules in CD47−/− mice because WT and CD47−/− Th1 cells express identical levels of LFA-1, VLA-4, and P-selectin glycoprotein ligand-1 (PSGL-1) and similar levels of intracellular IFN-γ, the Th1 signature cytokine (Figure 1, C and D). We routinely verified the absence of CD47 expression in CD47−/− T-cells (Figure 1C).

CD47 regulates Th1 effector cell adhesion and transmigration in vitro

To further delineate the adhesion defect in CD47−/− T-cells, we monitored adhesion and TEM of WT and CD47−/− Th1 cells on WT and CD47−/− murine heart endothelial cell (MHEC) monolayers by live-cell videomicroscopy in an in vitro flow model (Alcaide et al., 2012). WT Th1 cells arrested, and subsequently ~30% of adherent cells transmigrated across TNF-α–activated WT monolayers (Figure 2, A and B). As we would predict from the in vivo studies, CD47−/− Th1 cells exhibited reduced adhesion and TEM across WT endothelium compared with WT Th1 cells. CD47−/− T-cells also showed reduced adhesion and TEM across CD47−/− MHEC monolayers. Of interest, WT Th1 cells also exhibited significantly reduced adhesion and TEM across CD47−/− MHECs, indicating that endothelial cell CD47 also plays a role in TEM. Analysis of MHECs isolated from CD47−/− and WT mice showed essentially identical levels of surface-expressed PECAM-1 and ICAM-2 at baseline and similar levels of ICAM-1, VCAM-1, and E-selectin expression at baseline and after 4 h of TNF-α treatment (Figure 2C). These in vivo and in vitro studies indicate that expression of CD47 in both T-cells and endothelium is required for normal Th1 cell adhesion and TEM of TNF-α–inflamed endothelium. Here we focus on the role that CD47 expressed on T-cells plays in leukocyte recruitment.

### CD47 regulates Th1 cell adhesion to immobilized ICAM-1 and VCAM-1

CD47 associates with and regulates the adhesive functions of reticulocyte-expressed α4β1 integrins (Brittain et al., 2004), but no study examined whether CD47 regulates αLβ2 (LFA-1) integrin adhesive interactions with its endothelial ligand ICAM-1. We therefore studied the adhesion of WT and CD47−/− Th1 cells to ICAM-1-Fc coimmobilized with CXCL12 (SDF-1α) chemokine under flow conditions (Alcaide et al., 2012). WT Th1 cells arrested on ICAM-1, whereas CD47−/− Th1 cells showed a significant reduction in arrest (Figure 3A). Of note, the greatest relative reduction occurred at the highest shear stress level examined. This assay was repeated using immobilized VCAM-1-Fc molecules without chemokine because T-cells constitutively express VLA-4 integrins capable of binding VCAM-1 under flow conditions (Chen et al., 1999). A significant defect in CD47−/− Th1 cell arrest to VCAM-1 was observed at high shear stress levels but not at the lowest shear stress tested (Figure 3B). There were no differences between WT and CD47−/− Th1 cell accumulation on immobilized E-selectin, suggesting that induction of Th1 selectin ligand expression was not affected (Figure 3C). Taken together, the data suggest that CD47 in Th1 cells plays an important role in the function of LFA-1 and VLA-4 integrins required for adhesion to their endothelial cell ligands.

CD47 does not regulate LFA-1 adhesion-strengthening ICAM-1

Because CD47−/− Th1 cells showed a larger defect in adhesion to ICAM-1 compared with VCAM-1, we focused on LFA-1 and determined whether adhesion strengthening to ICAM-1, termed avidity regulation, was affected. Accordingly, we compared the ability of adherent WT and CD47−/− Th1 cells to resist detachment

Genotype	Number of mice	Number of vessels	Vessel diameter (µm)	Wall shear rate (s^{-1})	V_{crit} (µm/s)
WT	5	11	36 ± 2	844 ± 73	622 ± 52
CD47$^{-/-}$	4	5	43 ± 2	706 ± 145	533 ± 109

TABLE 1: Microvessel parameters.
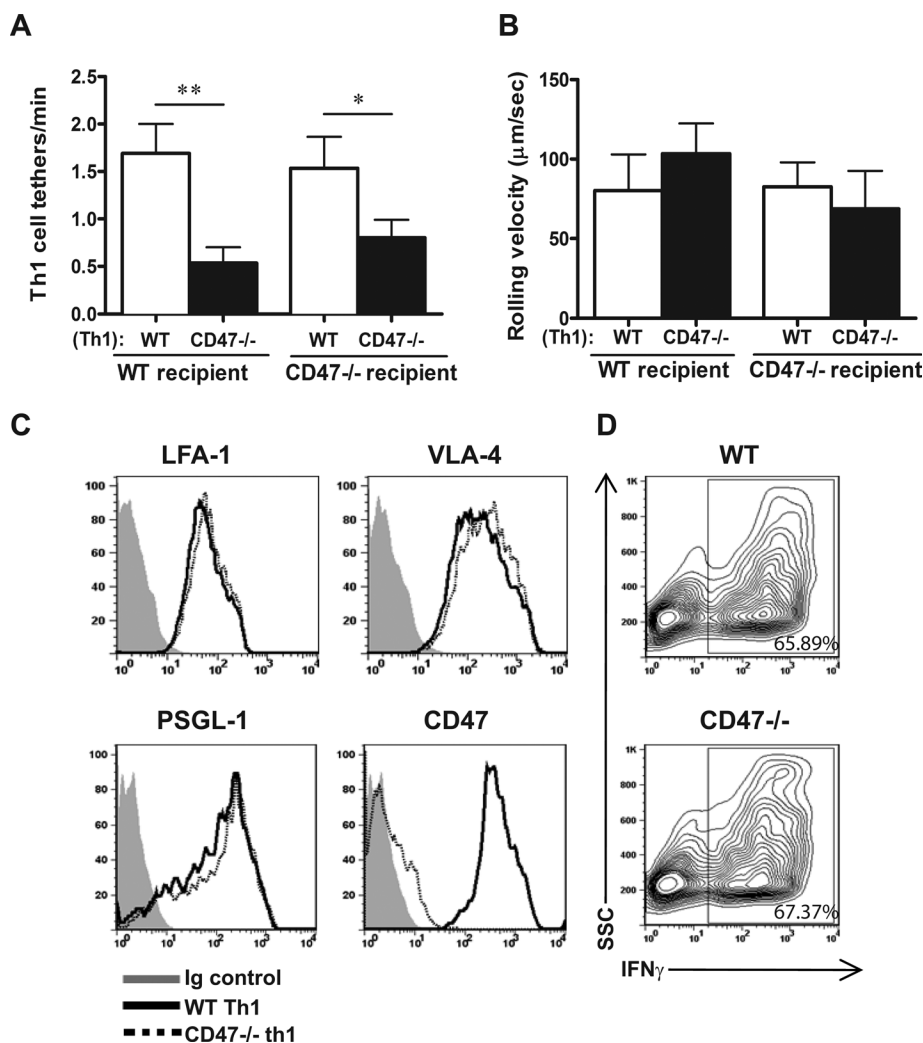
FIGURE 1: Adhesive interactions of Th1 effector cells with inflamed murine cremaster muscle microcirculation. (A) Impaired interaction of CD47$^{-/-}$ Th1 effector cells with TNFα-activated microvessels of the cremaster muscle. Tethered cells are defined as labeled Th1 cells that are stably bound to the inflamed vessel wall for more than three consecutive video frames (~2 s). Data are means ± SEM from five WT and CD47$^{-/-}$ recipient mice (13 vessels in WT and 7 vessels in CD47$^{-/-}$ mice). *$p < 0.05$ vs. WT Th1 in CD47$^{-/-}$ recipient; **$p < 0.01$ vs. WT Th1 in WT recipient (Student's t test). (B) Rolling Th1 cells are defined as T-cells that interact with the vessel below V_{crit}. Th1 cell rolling velocities were determined by measuring the length of time required to travel 200 µm. Velocities from three independent preparations of Th1 cells were analyzed in vessels from WT or CD47$^{-/-}$ mice. Tethered and rolling T-cells were identified in videos using Imaris software (Bitplane, Zurich, Switzerland). (C) WT and CD47$^{-/-}$ CD4$^+$ Th1 effector cells have essentially the same surface expression levels of LFA-1, VLA-4, and PSGL-1. (D) Intracellular staining shows that IFN-γ production is similar in polarized WT (66% positive) and CD47$^{-/-}$ (68% positive) Th1 cells.

from ICAM-1 immobilized with CXCL12 under increasing flow rates (Sircar et al., 2007). Whereas the number of CD47$^{-/-}$ Th1 cells initially bound under the lowest shear flow setting was 31% lower than with WT (264 ± 86 cells/mm^2 for WT adhesion vs. 182 ± 60 cells/mm^2 for CD47$^{-/-}$, $p < 0.05$, Student's t test), no

difference in the rate of cell detachment was detected upon applying the shear flow regime (Figure 3D). This finding demonstrates that CD47 is not necessary for postadhesion LFA-1 adhesion strengthening to ICAM-1.

CD47-null human T-cells phenocopy the defects in murine CD47$^{-/-}$ Th1-cell adhesion

An earlier study reported that human Jurkat T-cell clone JINB8 lacking CD47 (CD47$^-$) showed reduced binding to a TNF-α–stimulated human endothelial-like cell line as compared with the parental clone expressing CD47 (CD47$^+$; Ticchioni et al., 2001). Accordingly, we evaluated their adhesion to TNF-α–activated human umbilical vein endothelial cells (HUVECs) and immobilized ICAM-1 and VCAM-1. Both Jurkat clones express similar surface levels of LFA-1 and VLA-4 α-subunits and the respective common β2 and β1 integrin subunits (Figure 4A). CD47$^+$ Jurkat cells showed significantly greater adhesion to 4-h TNF-α–activated HUVEC monolayers than did CD47$^-$ cells at each shear stress tested (Figure 4B). Of interest, the dominant integrin responsible for T-cell adhesion was VLA-4 as determined by function-blocking monoclonal antibody (mAb) studies (Figure 4C), which is consistent with earlier studies (Chen et al., 1999; Ticchioni et al., 2001). Blocking LFA-1 on CD47$^+$ Jurkat cells reduced adhesion to similar levels as unblocked CD47$^-$ Jurkat cells. Blockade of LFA-1 on CD47$^-$ Jurkat cells did not further reduce adhesion to HUVECs. The lesser role of LFA-1 in Jurkat T-cell adhesion to HUVECs is likely the reason that Jurkat CD47$^-$ T-cell adhesion is not reduced to a greater level, as we would have predicted (Figure 4C).

We next evaluated Jurkat T-cell adhesion to immobilized ICAM-1, VCAM-1, and E-selectin under the same conditions as in Figure 3. CD47$^-$ T-cells showed significantly reduced stable arrest to both ICAM-1 and VCAM-1 compared with CD47$^+$ cells (Figure 5, A and B). The defects in arrest were most pronounced on ICAM-1 compared with VCAM-1, whereas there was no defect in adhesion to E-selectin (Figure 5C). As a control, we created stably transfected CD47$^-$ Jurkat cells expressing full-length CD47 tagged with green fluorescent protein (GFP; CD47+GFP) or GFP alone (CD47$^-$GFPcont).
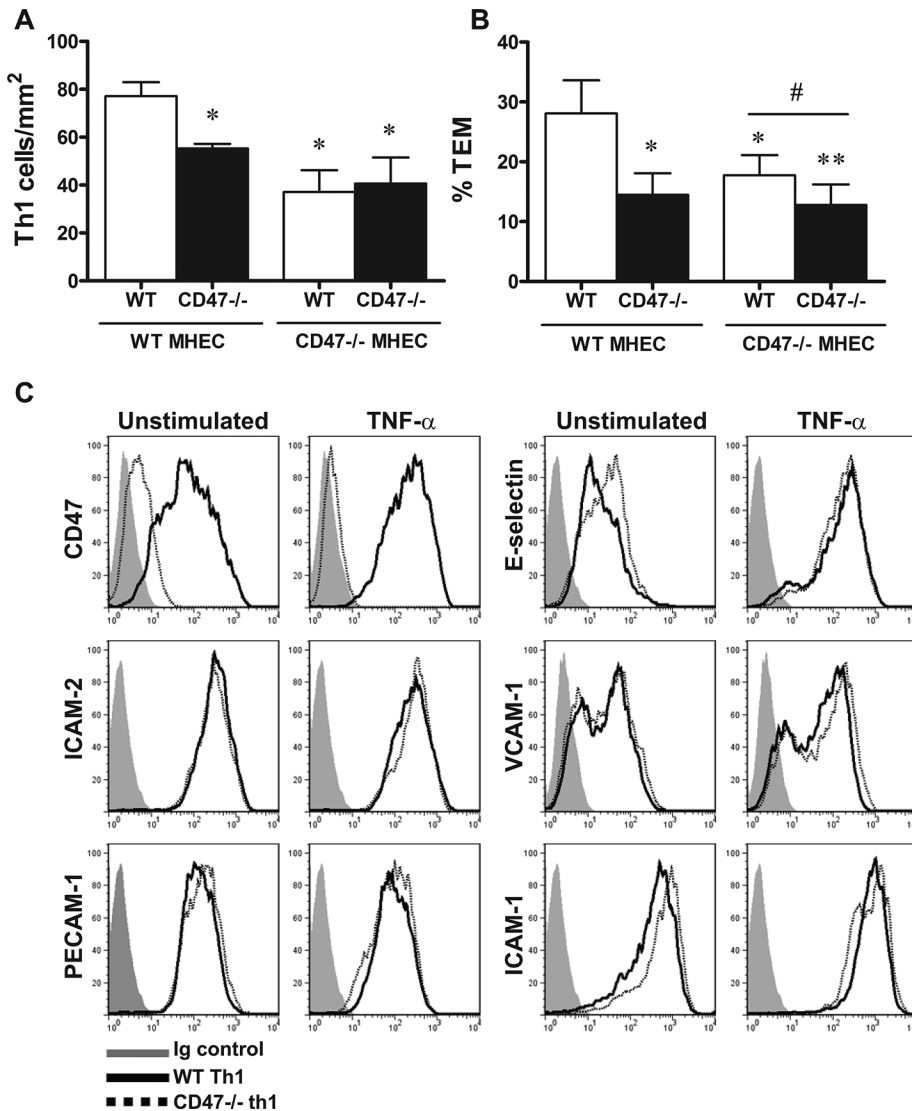
FIGURE 2: Th1 effector T-cell interactions with TNF-α–activated murine endothelium in an in vitro flow chamber. (A) The numbers of accumulated and (B) transmigrated T-cells in the videos were quantified by ImageJ software (National Institutes of Health, Bethesda, MD). Data are mean ± SEM. $*p \leq 0.05$ and $**p \leq 0.01$ vs. WT Th1 cell on WT MHEC. $\#p \leq 0.05$ are WT Th1 vs. CD47$^{-/-}$ on CD47$^{-/-}$ MHEC (Student's t test), $n = 3$ separate experiments. (C) MHECs were treated with medium or medium containing murine TNF-α (100 ng/ml) for 4 h, and CD47, VCAM-1, ICAM-1, E-selectin, ICAM-2, and PECAM-1 expression levels were detected by unlabeled primary mAb followed by staining with a PE-labeled goat anti-rat secondary mAb. Cell fluorescence was determined by FACSCalibur flow cytometry (BD, Franklin Lakes, NJ). Representative histograms of surface expression of molecules are shown from 10 separate experiments.

CD47 regulates β1 and β2 high-affinity conformations in response to Mn^{2+} or Mg^{2+}/ethylene glycol tetraacetic acid

Integrin affinity regulation was evaluated on Jurkat CD47$^-$ and CD47$^+$ cells by reporter mAbs that detect activated conformations of β1 and β2 integrins. KIM127 mAb detects and stabilizes an extended and closed conformation of β2 integrins (intermediate affinity), and mAb 24 recognizes an extended and open "active" conformation of β2 integrins (high affinity; (Salas et al., 2004). Jurkat T-cells express predominantly LFA-1 (αLβ2) and not the other α-subunit chains that associate with β2 integrins, and hence these mAbs to β2 integrins detect primarily the intermediate- and high-affinity conformations of LFA-1 (Salas et al., 2004). HUTS21 detects and stabilizes activated β1 integrins (Luque et al., 1996), and we showed previously that expression of this epitope correlated with robust adhesion of human memory T-cells to VCAM-1 (Lim et al., 2000). As expected, incubation of CD47$^+$ T-cells with Mn^{2+} or Mg^{2+}/ethylene glycol tetraacetic acid (EGTA), global activators of integrins, triggered robust expression of both intermediate- and high-affinity LFA-1 (Figure 6, A and B). In contrast, CD47$^-$ T-cells showed a significantly reduced expression of intermediate- and high-affinity conformations of LFA-1 in response to Mn^{2+} or Mg^{2+}/EGTA. It is unlikely that this assay did not detect transient LFA-1 activation because the mAbs stabilize the active conformation and were present throughout the assay. In addition, failure to detect mAb expression was not due to a change (loss) in total surface expression of β1 or β2 integrins upon exposure to Mn^{2+} or Mg^{2+}/EGTA (Figure 6C). CD47$^-$ T-cells also showed reduced induction of high-affinity β1 integrins versus CD47$^+$ T-cells after treatment with Mn^{2+} or Mg^{2+}/EGTA buffers (Figure 6D). Consistent with the failure of Mn^{2+} or Mg^{2+}/EGTA treatments to induce intermediate- and high-affinity LFA-1 conformations in the absence of CD47, CD47$^-$ T-cells exhibited little binding of soluble ICAM-1-Fc versus CD47$^+$ T-cells (Figure 6E). In addition, treatment of CD47$^-$ cells with Mn^{2+} did not restore binding comparable to CD47$^+$ T-cell adhesion to either immobilized ICAM-1 or VCAM-1 under flow (Supplemental Figure S1, A and B). Taken together, the results indicate that CD47 expression is required for expression of intermediate- and high-affinity conformations of LFA-1 and for binding soluble ICAM-1, as well as for induction of activated β1 integrins.

To determine whether β2 integrins in CD47$^-$ cells could be activated when extracted from the membrane milieu of CD47$^-$ Jurkat T-cells, we examined the effect of 1.0 mM Mn^{2+} on β2 integrins in the soluble phase. When detergent lysates of CD47$^+$ and CD47$^-$ T-cells were incubated in the presence of Mn^{2+} and mAb24 to immunoprecipitate activated β2 integrins, an equal and robust
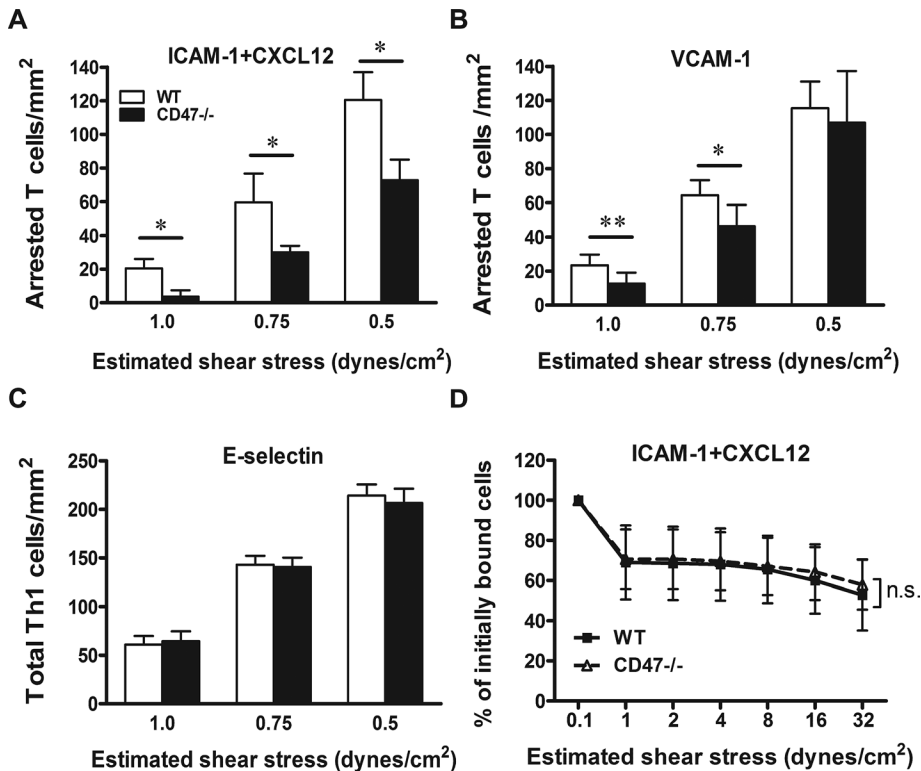
The level of CD47 expression was similar to that for the parental clone (data not shown) and restored arrest to ICAM-1 to a level similar to that for the parent clone, whereas CD47$^-$GFP-cont cell adhesion did not improve (Figure 5D). Finally, we examined the adhesion-strengthening capability of CD47$^+$ and CD47$^-$ Jurkat T-cells, using a detachment assay. CD47$^-$ Jurkat T-cells also exhibited 35% reduction in initial binding under the lowest shear stress conditions (211 ± 24 cells/mm^2 for CD47$^+$ adhesion vs. 137 ± 24 cells/mm^2 for CD47$^-$; $p < 0.05$) but no defect in the rate of detachment versus CD47$^+$ cells (Figure 5E), which is consistent with the behavior of murine CD47$^{-/-}$ Th1 cells (Figure 3D).

FIGURE 3: CD47^{−/−} Th1 cells have impaired adhesion to immobilized ICAM-1 and VCAM-1 but not E-selectin in an in vitro flow chamber model. WT and CD47^{−/−} Th1 cells were drawn across immobilized ICAM-1-Fc (A), VCAM-1-Fc (B), and E-selectin-Fc chimeric proteins (C) at the shear stress levels indicated, and cell adhesion was determined as detailed in *Materials and Methods*. Data are mean ± SEM, $n = 3$. *$p \leq 0.05$, **$p \leq 0.01$ (Student's *t* test). (D) Shear flow–mediated detachment of Th1 cells prebound to immobilized ICAM-1 + CXCL12 is not altered in CD47^{−/−} Th1 cells. Data are mean ± SEM, $n = 3$ separate experiments.

signal was detected in the absence and presence of CD47 (Figure 6F, lanes 3 and 6). mAb 24 did not immunoprecipitate β2 integrins in either cell type in the absence of Mn^{2+} (lanes 2 and 5). As a control, immunoprecipitation with mAb TS1/18, which recognizes all conformations of β2 integrin, is shown in lanes 1 and 4. These data indicate that CD47 is required for full activation of β2 integrins in the plasma membrane milieu of human T-cells but not with detergent-solubilized β2 integrins.

CD47 interacts with β2 integrin

Prior studies reported that VLA-4 coimmunoprecipitated with CD47 in blood reticulocytes from sickle cell patients (Brittain *et al.*, 2004). To evaluate whether CD47 associates with β2 integrins in T-cells, we applied fluorescence lifetime imaging microscopy (FLIM), a quantitative method for determining Förster resonance energy transfer (FRET; Table 2 and Figure 7A), to study whether β2 integrin and CD47 are sufficiently close to imply a physical interaction. Epifluorescence images were captured as quality control of the staining (Figure 7B). The lifetime of the donor molecule (τ_1; picoseconds), in this case β2 integrin, labeled with Alexa Fluor 488–conjugated secondary antibody was determined first in the absence of an acceptor fluorophore (Table 2 and Figure 7A, donor only). FRET between the donor fluorophore (β2 integrin) and acceptor (CD47 directly labeled with Alexa Fluor 594) was defined by the lifetime of interacting molecules (τ_1), with a_1 (in percent) defining the fraction of interacting molecules. The significant decrease of τ_1 (and also the mean lifetime, τ_m) for β2 integrin–CD47 indicates a close association between

β2 integrin and CD47, and the a_1 value indicates that 31.7 ± 4.1% of β2 integrin molecules interact with CD47 on the cellular membrane of Jurkat T-cells (Table 2). For comparison purposes the noninteracting molecules β2 integrin and PSGL-1 were costained as donor and acceptor molecules, respectively. A decrease of τ_1 was found when PSGL-1 was used as acceptor, but the interacting fraction was only 13.3 ± 1.5% and approached the lower levels of sensitivity. Furthermore, the τ_m of the donor was unchanged in the presence of the acceptor, indicating that β2 integrin and PSGL-1 were not in sufficient proximity to support a physical interaction (Supplemental Table S1 and Supplemental Figure S2A). As a positive control a decrease in τ_1 was observed between LFA-1 α-chain (αL integrin) and the common β2 chain (Supplemental Table S1 and Supplemental Figure 2A). Representative histograms illustrate the τ_m of the donor β_2 integrin in the different conditions (Supplemental Figure S3, A–F). These results support a direct association of CD47 with β2 integrins.

We next asked whether the CD47–β2 integrin association was altered upon incubation of T-cells with Mg^{2+}/EGTA–containing medium, using the same donor and acceptor antibodies. Of interest, there was no change in τ_1 (and τ_m) for β2 integrin–CD47, still indicating a close association between β2 integrin and CD47. The a_1 values, however, indicate that significantly fewer β2 integrin molecules interact with CD47 (Table 2). This decrease in association was not due to a change (loss) in total surface expression of β1 or β2 integrins upon exposure to Mn^{2+} or Mg^{2+}/EGTA (Figure 6C). We next explored whether the extended or fully activated β2 integrin conformations interact with CD47 by staining cells with mAb 24 and KIM127 incubated in medium containing Mg^{2+}/EGTA or medium alone. Under conditions of medium with Mg^{2+}/EGTA or medium alone, we were unable to detect a signal above background for the extended conformation (KIM127). Although the signal for the fully activated β2 integrin (mAb 24) was also too low to detect in medium alone, the signal was clearly detected in cells incubated in medium containing Mg^{2+}/EGTA. Reduced τ_1 (and τ_m) for β2 integrin–CD47 indicates close association between activated β2 integrins and CD47, and the a_1 value indicates that 28 ± 1% of activated β2 integrin molecules interact with CD47 on the cellular membrane of Jurkat T-cells (Table 3). These data indicate that the fully activated β2 integrins do interact with CD47, but the results do not distinguish whether the fraction of fully activated integrins associated with CD47 increases or decreases upon cation-induced integrin activation.

DISCUSSION

CD47 associates with and regulates α4β1 integrins in reticulocytes (Brittain *et al.*, 2004). On the basis of this report and our findings that mouse T-cell recruitment requires CD47 expression in a dermal air pouch model of inflammation (Azcutia *et al.*, 2012), we used molecular imaging analysis, in vitro flow chamber adhesion assays, and in
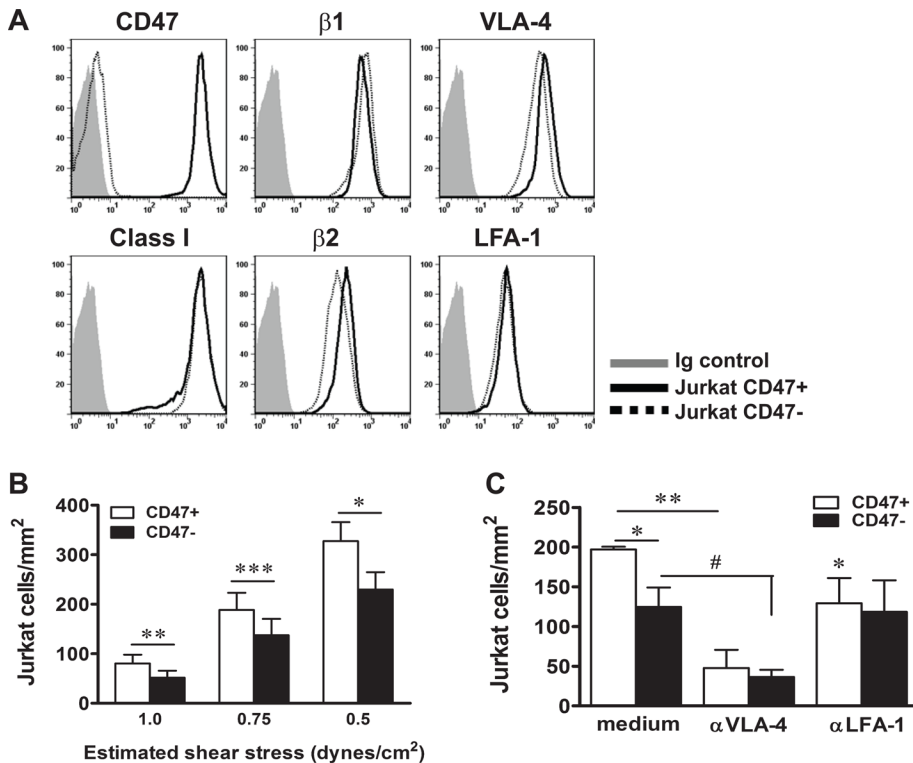
FIGURE 4: Human Jurkat T-cell integrin expression and adhesion to HUVEC monolayers in an in vitro flow model. (A) Jurkat CD47+ clone E6 and CD47− (null) clone JINB8 express similar levels of LFA-1 and VLA-4 integrins. Data are representative of three separate experiments. (B) Jurkat CD47− T-cells were drawn across the TNF-α–activated HUVECs at various estimated shear stress levels as described in *Materials and Methods*. *$p \leq 0.05$, **$p \leq 0.01$, ***$p \leq 0.001$ for indicated comparisons (Student's t test). (C) Both CD47+ and CD47− Jurkat T-cell adhesion (under shear stress of 0.76 dynes/cm²) to TNF-α–activated HUVECs is strongly dependent on VLA-4 integrins. The reduction in adhesion in CD47+ cells with blockade of LFA-1 is not observed in CD47− cells, suggesting that LFA-1–dependent adhesion requires CD47. Data are mean ± SEM of three experiments. *$p \leq 0.05$, **$p \leq 0.01$ vs. CD47+ with no mAb in medium; #$p < 0.05$, media CD47− vs. anti-VLA-4 mAb–treated CD47− cells (Student's t test).

examined previously (Ticchioni *et al.*, 2001), using the same Jurkat T-cell lines used here. These authors reported that CD47− Jurkat T-cells had reduced adhesion to TNF-activated endothelium and to immobilized VCAM-1. Our present data extend this finding to include a striking defect in LFA-1 adhesive function.

We also performed detachment assays to quantify LFA-1 adhesion strengthening to ICAM-1 in CD47− cells. Adhesion strengthening occurs after integrin activation and initial ligand binding and involves avidity regulation, defined as clustering or increased mobility of integrins in the plasma membrane of adherent cells (Kim *et al.*, 2004). In contrast to the defects in arrest, the assay revealed no differences in detachment of adherent T-cells that lacked CD47. This suggests that the absence of CD47 affects affinity regulation of LFA-1 but not avidity regulation.

CD47 is required for LFA-1 and VLA-4 high-affinity conformation expression

LFA-1 is predicted to assume at least three distinct conformational states: a bent structure with low affinity for ligand, an extended and closed headpiece structure with intermediate affinity, and an extended and open headpiece structure with high affinity (Hogg *et al.*, 2011; Lefort *et al.*, 2012). Recent studies report that the high-affinity LFA-1 conformation is required for T-cell arrest and adhesion to ICAM-1 expressed by endothelium or binding soluble ICAM-1 (Constantin *et al.*, 2000; Salas *et al.*, 2004; Shamri *et al.*, 2005; Smith *et al.*, 2005). Mn^{2+} or Mg^{2+}/EGTA

vivo studies to investigate whether the defect in T-cell recruitment was related to impaired β1 and β2 adhesive functions in the absence of CD47. Indeed, our key observation is that CD47 is necessary to induce high-affinity conformations of LFA-1 and VLA-4 in T-cells.

CD47 regulates LFA-1 and VLA-4 adhesive functions under shear flow conditions

Effector T-cell arrest, migration, and transendothelial migration require VLA-4 and LFA-1 integrin activation and binding to their endothelial ligands VCAM-1 and ICAM-1. Our present data show that murine CD47−/− Th1 effector cells, as compared with WT, have reduced adhesive interactions with inflamed cremaster microvessels and reduced adhesion and transmigration across TNF-α–activated endothelium. These defects can be explained by our data showing that CD47−/− Th1 cells have reduced adhesion to immobilized VCAM-1 and ICAM-1 but not E-selectin. This result implies that CD47−/− Th1 cells have impaired β1 and β2 integrin adhesive functions. Accordingly, the use of human Jurkat T-cells that lack CD47 showed striking defects in integrin-dependent adhesion identical to murine CD47−/− Th1 cells. Thus we conclude that CD47 expression plays a critical role in LFA-1 and VLA-4 binding to ICAM-1 and VCAM-1 under flow conditions in vivo and in vitro. The role of CD47 in regulation of VLA-4 adhesion under shear flow conditions was

treatments bypass inside-out signaling and trigger high-affinity β1 and β2 conformations and rapid ligand binding (Shimaoka *et al.*, 2002). Indeed, CD47+ T-cells exhibit a robust response to these stimuli and avidly bind integrin activation reporter mAbs KIM127, 24, and HUTS21. A notable and unanticipated result was that high-affinity conformations in β2 integrins, and to a lesser extent β1 integrins, were only modestly induced by Mn^{2+} or Mg^{2+}/EGTA in CD47− Jurkat T-cells. In addition, Mn^{2+} treatment of CD47− cells failed to restore their adhesive function to immobilized ICAM-1 and VCAM-1. Because we observed more-severe defects in LFA-1 versus VLA-4 function in CD47− T-cells, we chose to study a possible novel CD47 regulation of LFA-1 in more detail. In a second readout of LFA-1 activation, soluble ICAM-1 binding was also dramatically reduced in CD47− T-cells. Our results suggest that CD47 directly or indirectly facilitates and/or stabilizes activated forms of LFA-1. To our knowledge this is the first report to demonstrate in leukocytes a requirement for a second transmembrane protein to achieve high-affinity LFA-1 conformations. This effect of CD47 on LFA-1 activation occurred only in intact cell membrane microenvironment because β2 integrins solubilized from CD47+ or CD47− cells could be activated by Mn^{2+}. Further studies are necessary to identify the molecular mechanism of CD47 interactions with and regulation of leukocyte β and β2 integrin binding affinity. Previous studies, however, shed some light on this topic. In VLA-4–expressing reticulocytes isolated
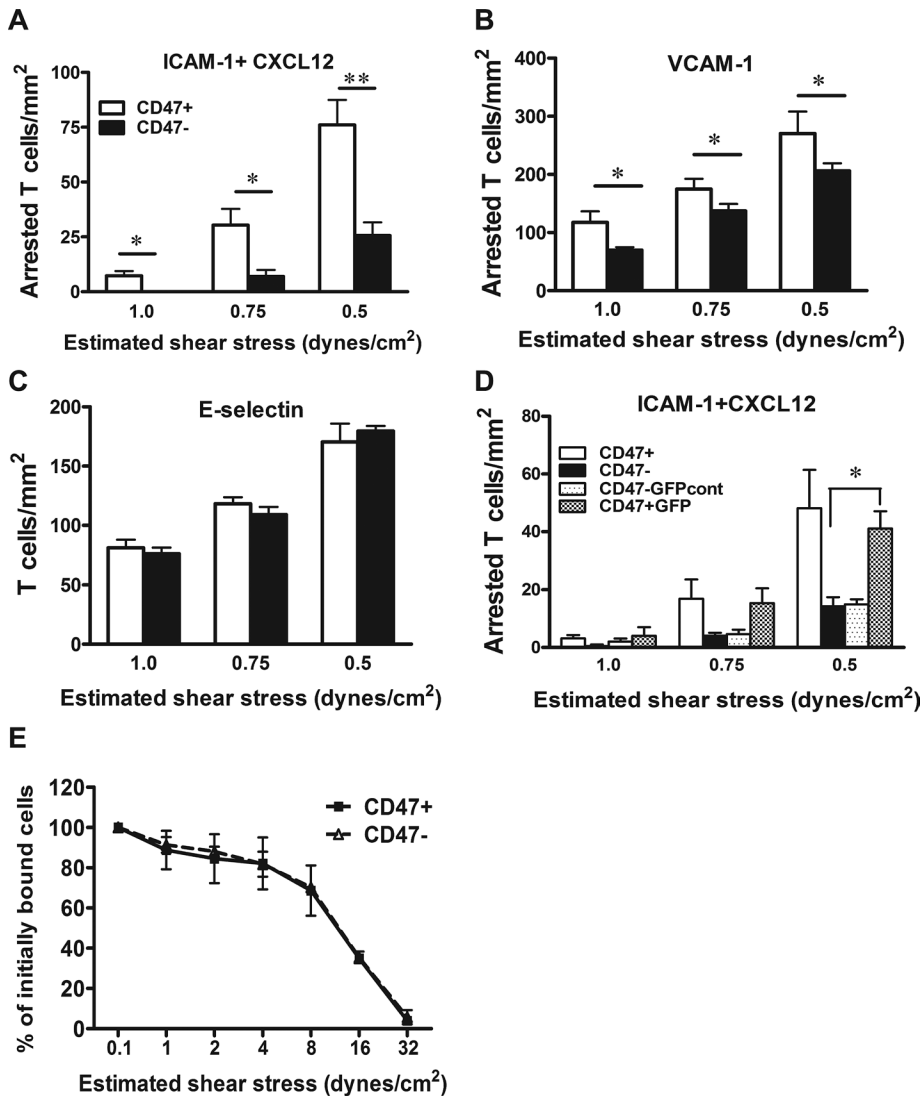
FIGURE 5: Jurkat CD47$^-$ (null) T-cells have impaired adhesion to immobilized ICAM-1 and VCAM-1 but not E-selectin under shear flow conditions. (A–C) Jurkat T-cells were drawn across immobilized ICAM-1 (A), VCAM-1 (B), or E-selectin (C) proteins at various shear stress levels, and adhesion was measured as described in *Materials and Methods*. (D) Transfection of CD47$^-$ Jurkat cells with a plasmid containing CD47 tagged with GFP (CD47 + GFP) rescued cell adhesion to ICAM-1. In contrast, transfection of CD47$^-$ cells with a plasmid containing only GFP (CD47-GFPcontrol) did not. (E) Detachment of Jurkat T-cells prebound to immobilized ICAM-1 is not affected by the absence of CD47. Data are means ± SEM of at least three independent experiments. *$p \leq 0.05$, **$p \leq 0.01$ (Student's t test).
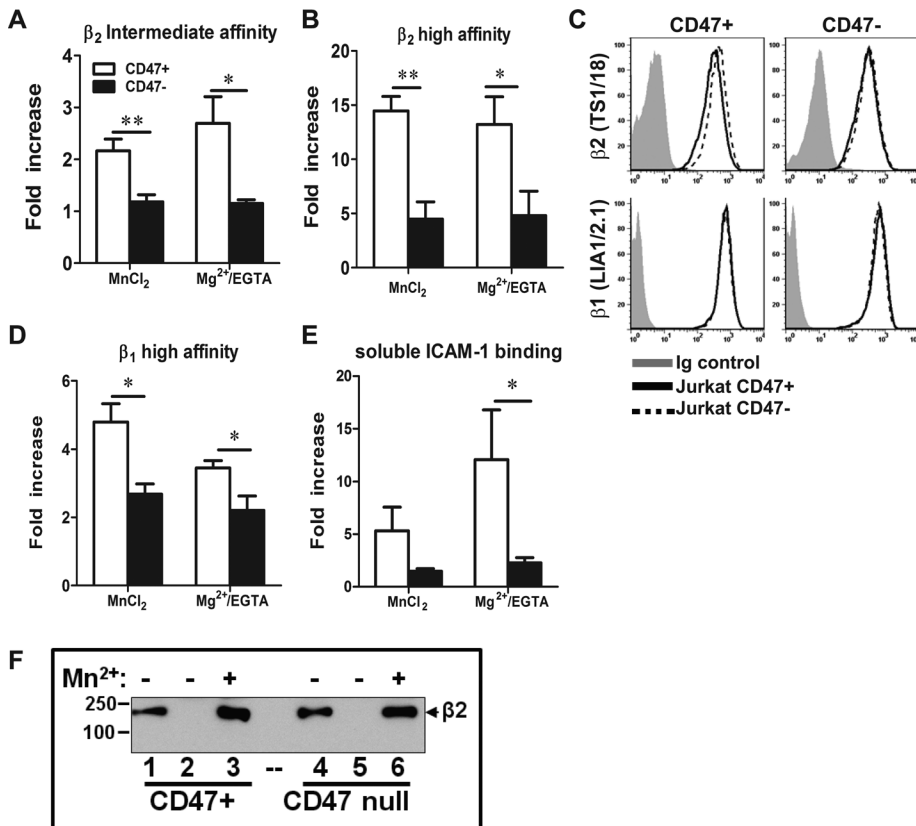
Jurkat T$^-$ cells (Table 2). FLIM studies performed on T-cells in medium that activates β2 integrins suggest that β2 integrins remain associated with CD47 and that the percentage of interacting molecules was significantly reduced. Parallel studies with mAb 24, which detects fully activated β2 integrins, confirm that activated integrins associate with CD47; however, comparison of the fraction of activated β2 integrins that associate with CD47 at rest and upon activation could not be determined. Further studies are necessary to explore the spatial and temporal interactions between CD47 and β1 and β2 integrins during leukocyte adhesive interactions with VCAM-1 and ICAM-1 and with activated endothelium. We speculate that CD47 plays a role in regulating high-affinity conformations of integrins in other leukocyte types, based on our report that recruitment of neutrophils, CD3$^+$ T-cells, and monocytes is significantly reduced in a dermal air pouch model in CD47$^{-/-}$ mice (Azcutia et al., 2012). It is also likely that the results reported here for CD47 regulation of LFA-1 and VLA-4 explain, in part, the reduced leukocyte recruitment and level of inflammation in CD47$^{-/-}$ mice reported previously (Lindberg et al., 1996; de Vries et al., 2002; Su et al., 2008; Azcutia et al., 2012).

In summary, our results indicate that CD47 in *cis* interactions regulate LFA-1 and VLA-4 integrin affinity, and in turn, this process plays a substantial role in the adhesion and diapedesis of T-cells in models of inflammation. From our present results we infer the existence of a distinct and perhaps novel pathway that regulates T-cell recruitment in vivo to sites of inflammation, and we identify a potential therapeutic target for the treatment of immune-mediated diseases.

MATERIALS AND METHODS
Materials
Recombinant human and mouse E-selectin, VCAM-1, and ICAM-1 Fc-chimeras were from R&D Systems (Minneapolis, MN). Recombinant mouse interleukin-2 (IL-2), IL-12, and TNF-α were purchased from BioLegend (San Diego, CA). The following hybridoma clones were purchased from the American Type Culture Collection, Manassas, VA) and used as purified IgG: mAbs to β2 integrins include KIM127 (Andrew et al., 1993) and TS1/18 (Miller et al., 1986); TS1/22 recognizes LFA-1 (Miller et al., 1986); B6H12 and 2D3 are functional blocking and nonblocking, respectively, and recognize human CD47 (Brown et al., 1990). 13A9 recognizes a functional epitope in PSGL-1 (Snapp et al., 1997); mAb 24 was provided by Nancy Hogg (Cancer Research Institute, London, United Kingdom; Dransfield and Hogg, 1989); HUTS 21, LIA1/2.1, and HP2/1 were provided by Francisco Sanchez-Madrid (Hospital de la Princesa, Madrid, Spain; Lim et al., 2000); rabbit polyclonal anti-CD18 was described previously (Quinn et al., 2001); and mAb to mouse CD47 (miap301) was from eBiosciences (San Diego, CA). mAb to mouse

from sickle cell disease patients, CD47 coimmunoprecipiated with β1 integrins and regulated VLA-4–dependent adhesion to VCAM-1 and TSP-1 (Brittain et al., 2004). Other reports used various CD47 chimeric molecules expressed in Jurkat CD47$^-$ cells to demonstrate that only the extracellular IgV and first transmembrane domains of CD47 were required to restore Jurkat T-cell arrest on VCAM-1 (Ticchioni et al., 2001). A similar strategy in a CD47$^-$ ovarian cancer cell line demonstrated that expression of the IgV domain linked to GPI was sufficient to promote clustering of αvβ3 and binding of activation-sensing LIBS1 and LIB6 mAb (McDonald et al., 2004). Our FLIM-FRET analyses support a direct in *cis* association between CD47 and β2 integrins in Jurkat T-cells. The significant decrease of both τ_m and τ_1 for β2 integrin–CD47 supports the conclusion of a close association between β2 integrin and CD47, and the a_1 value indicates that ~32% of β2 integrin molecules interact with CD47 in

FIGURE 6: Mn²⁺ or Mg²⁺/EGTA fails to induce strong LFA-1 and β1 high-affinity conformation expression or binding of soluble ICAM-1-Fc chimera in CD47⁻ (null) Jurkat T-cells. (A–D) Mn²⁺ or Mg²⁺/EGTA–induced expression of LFA-1 extended and open "activated" conformations of LFA-1 were detected by the reporter mAb KIM127 (A) and mAb24 (B). Results are normalized to isotype-matched, control nonbinding mAb. Expression of these active conformations of integrins by 0.5 mM Mn²⁺ or 10 mM Mg²⁺/1 mM EGTA treatments was significantly reduced in CD47⁻ Jurkat T-cells. (C) Total levels of β2 and β1 integrins detected with TS1/18 and LIA1/2.1 mAb, respectively, did not change after Mn²⁺ or Mg²⁺/EGTA stimulation. No change was detected in CD47 (data not shown). (D) High-affinity β1 integrins induced by Mn²⁺ or Mg²⁺/EGTA buffer were measured by mAb HUTS21. (E) CD47⁻ T-cells exhibited little binding of soluble ICAM-1 as compared with CD47+ T-cells induced by Mn²⁺ and Mg²⁺/EGTA treatments. Results are normalized to incubation buffer alone. Data are mean ± SEM, n = 3. *p ≤ 0.05, **p ≤ 0.01 (Student's t test). (F) Mn²⁺ activates solubilized β2 integrins from CD47⁺ (lane 3) and CD47-null (lane 6) Jurkat T-cells. Lysates of Jurkat cells were subjected to immunoprecipitation with anti-β2 integrin mAb 24 (lanes 2, 3 and 5, 6) in the absence (–) or presence (+) of 1.0 mM Mn²⁺, followed by SDS–PAGE and immunoblotting with anti-β2 integrin polyclonal Ab (R&D Systems). Immunoprecipitation with mAb TS1/18 (lanes 1 and 4) served as a positive control to ensure the presence of β2 integrin in the lysate.

Research Building in accordance with the guidelines of the Committee of Animal Research at the Harvard Medical School and the National Institutes of Health animal research guidelines.

Cells

HUVECs were isolated and passaged as previously described and used at passage 2 for in vitro flow chamber assays (Stefanidakis et al., 2008). MHECs were prepared as described (Alcaide et al., 2012) from 8- to 12-d-old animals. Murine CD4⁺ Th1 effector cells were derived from naive T-cells by CD3 and CD28 stimulation in the presence of IL-12 and IFN-γ polarizing conditions as previously described (Alcaide et al., 2012). The human Jurkat T-cell E6.1 clone expressing CD47 (TIB-152) was from the American Type Culture Collection, and Jurkat T-cell clone E6.1 lacking CD47 (JINB8) was described previously (Ticchioni et al., 2001). Jurkat T-cells were maintained in RPMI-1640 supplemented with 10% fetal bovine serum (FBS), antibiotics, and L-GlutaMAX.

Flow cytometry

Flow cytometry analysis of intracellular IFN-γ was performed to corroborate the differentiation of Th1 cells and monitor expression of murine CD47, LFA-1, VLA-4, and PSGL-1 and also on human Jurkat T-cells using standard immunofluorescence staining and flow cytometry methods.

Intravital microscopy

In vitro polarized WT and CD47⁻/⁻ Th1 cells were labeled with different fluorescent dyes (CFSE or Alexa 680), and then 3 × 10⁶ of each cell type were mixed together and coinjected retrograde using a femoral artery catheter into WT or CD47⁻/⁻ recipient mice 2 h after TNF-α injection as described (Alcaide et al., 2012). Leukocyte–endothelial adhesive interactions were obtained with an Olympus FV 1000 intravital microscope (Center Valley, PA) equipped with a LumPlan 40×/0.8 numerical aperture (NA) water immersion objective and digitally recorded with an Olympus DP71 charge-coupled device video camera and Olympus FluoView 1000 imaging software. Rolling Th1 cells were identified as the visible cells passing through and transiently interacting with vessel surface in a plane perpendicular to the vessel axis. Rolling velocities were calculated as previously detailed (Alcaide et al., 2012). V_crit was calculated as described previously (Ley et al., 1995; Yang et al., 1999).

interferon (IFN)-γ, ICAM-1, ICAM-2, VCAM-1, PECAM-1, E-selectin, PSGL-1, LFA-1, and VLA-4 were purchased from BD PharMingen (San Jose, CA). Vibrant CFSE and Alexa 680 cell tracker, goat anti-mouse and anti-rabbit Alexa Fluor 488, and goat anti-mouse and anti-rabbit Alexa Fluor 594 secondary antibodies were from Invitrogen (Carlsbad, CA). Vectashield with 4′,6-diamidino-2-phenylindole (DAPI) was from Vector Laboratories (Burlingame, CA).

Mice

CD47-deficient (CD47⁻/⁻) mice (C57BL/6 strain) were obtained from Eric Brown (Genentech, South San Francisco, CA; Lindberg et al., 1996). WT C57BL/6 mice (Charles River Laboratories, Wilmington, MA) were used to establish a breeding colony in our facility for use as WT control animals. All mice used were bred in the same pathogen-free facility at Harvard Medical School New

T-cell adhesion to immobilized Fc chimera adhesion molecules and MHECs under defined laminar shear flow conditions in vitro

T-cell adhesion and transendothelial migration and interactions with immobilized adhesion molecules were performed as described

Condition	τ_1 (ps)	a_1 (%)	τ_m (ps)
β2 integrin (donor only)	2836 ± 11	100 ± 0	2836 ± 11
β2 integrin + CD47 (B6H12)	842.7 ± 137[a]	32 ± 4	2218 ± 136[a]
β2 integrin (donor only) + Mg^{2+}/EGTA	2889 ± 21.3	100 ± 0	2889 ± 21
β2 integrin + CD47 (B6H12) + Mg^{2+}/EGTA	804 ± 101[b#]	23 ± 1[c]	2442 ± 50[b#]

Values represent mean ± SEM for $n = 20$ for each condition.
[a]$p < 0.001$ β2 integrin–CD47 vs. β2 integrin donor only.
[b]$p < 0.001$ β2 integrin–CD47 + Mg^{2+}/EGTA vs. β2 integrin donor only + Mg^{2+}/EGTA.
[c]$p < 0.05$ β2 integrin–CD47 + Mg^{2+}/EGTA vs. β2 integrin + CD47 unstimulated.
[#]n.s., β2 integrin–CD47 + Mg^{2+}/EGTA vs. β2 integrin + CD47 unstimulated.

TABLE 2: FLIM analysis of total β2 integrin–CD47 interactions.

(Alcaide et al., 2012). Briefly, in vitro polarized WT and CD47$^{-/-}$ Th1 cells (5 × 10^5 in 100 µl) were suspended in Dulbecco's phosphate-buffered saline (PBS) containing 0.1% (vol/vol) bovine serum albumin and 20 mM 4-(2-hydroxyethyl)-1-piperazineethanesulfonic acid (HEPES), pH 7.4, and were drawn across WT or CD47$^{-/-}$ 4-h TNF-α–treated MHECs at 37°C in an in vitro flow chamber. Live-cell imaging of leukocyte TEM was performed using a digital imaging system coupled to a Nikon Eclipse Ti inverted microscope (Nikon, Melville, NY) equipped with a 20×/0.75 NA differential interference contrast objective. Time-lapse videos were acquired using MetaMorph software (Molecular Devices, Sunnyvale, CA). Polarized Th1 cells also were drawn across immobilized ICAM-1-Fc (20 µg/ml), VCAM-1-Fc (5 µg/ml), and E-selectin-Fc (20 µg/ml) chimeric proteins at estimated shear stress levels of 1.0, 0.75, and 0.5 dyn/cm^2 as previously detailed (Alcaide et al., 2012). Live-cell imaging of leukocyte adhesion was recorded by a video camera coupled to a Nikon TE2000 inverted microscope equipped with a 20×/0.75 NA phase contrast objective and VideoLab software (Mitov, Moorpark, CA).

Immunoprecipitation and blotting

CD47$^+$ and CD47$^-$ Jurkat cells were solubilized in cold lysis buffer (10 mM HEPES, pH 7.4, 150 mM NaCl, 100 mM octylglucoside, 1 mM phenylmethylsulfonyl fluoride, and 1× protease inhibitor cocktail [P8340; Sigma-Aldrich, St. Louis, MO]) and centrifuged at 100,000 × g for 30 min at 4°C. Lysates were divided and immunoprecipitated overnight at 4°C with protein A/G–Sepharose and mAb TS1/18, mAb 24, or mAb 24 and 1 mM Mn^{2+}, and proteins were separated by SDS–PAGE. The β2 integrin was detected by Western blot with goat anti-human β2 integrin polyclonal antibody (R&D Systems, Minneapolis, MN).

Epifluorescence and time-correlated single-photon counting FLIM analysis

Aliquots of Jurkat CD47$^+$ cells (3 × 10^5) were fixed in 4% paraformaldehyde and transferred to glass slides by Cytospin centrifugation (Shandon, Astmoor, England) and then
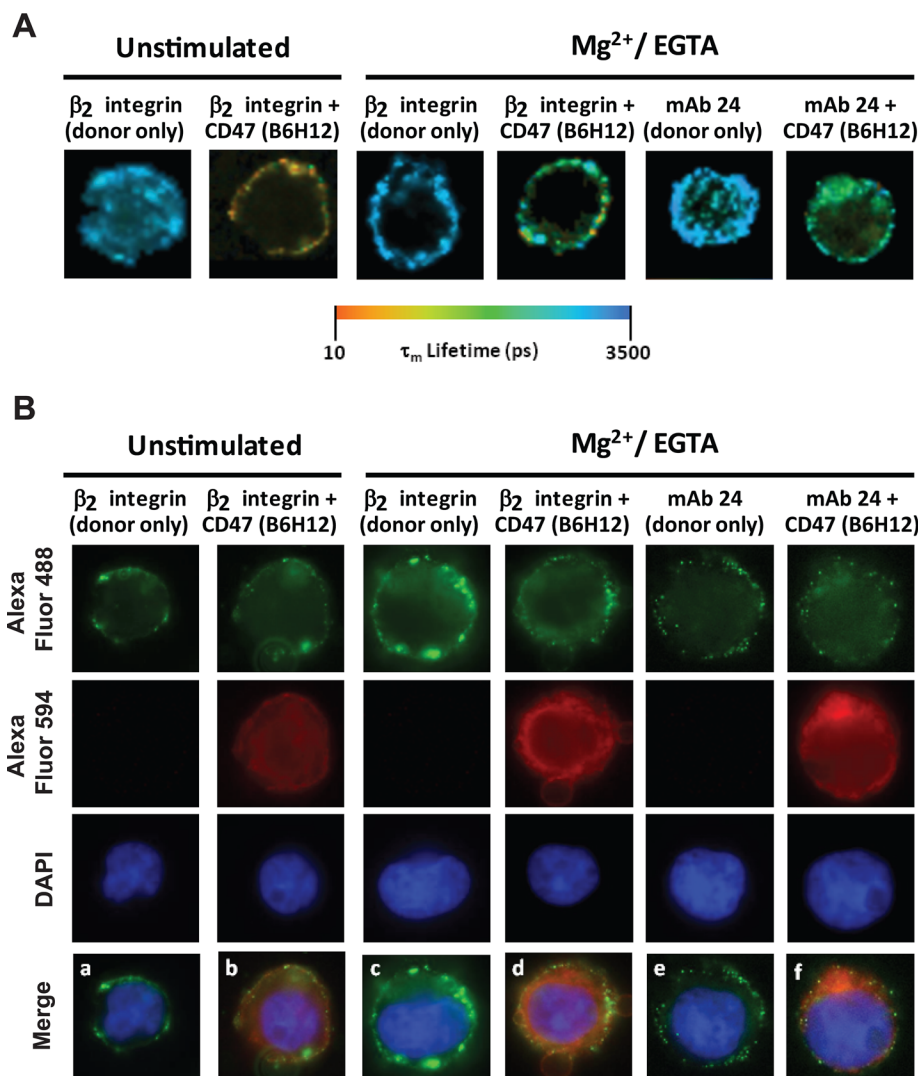

FIGURE 7: CD47 and β2 integrin interact on the cellular membrane of Jurkat T-cells. (A) Representation of interacting fraction τ_m by pseudocolor images of the FLIM-FRET analysis of the interaction between β2 integrins with CD47 in unstimulated conditions and upon Mg^{2+}/EGTA activation, and the interaction between activated β2 integrin detected by mAb 24 and CD47 upon integrin activation with Mg^{2+}/EGTA. The color scale for τ_m ranges from 10 to 3500 ps. The β2 integrin was identified with the donor fluorophore (Alexa Fluor 488) and CD47 with the acceptor fluorophore (Alexa Fluor 594). (B) Localization of β2 integrin and CD47 by epifluorescence. Fixed cells were stained with (a, c) anti-β2 integrin polyclonal antibody alone (Quinn et al., 2001), (b, d) anti-β2 integrin antibody and anti-CD47 (B6H12) antibody labeled with Alexa 594 (unstimulated or with Mg^{2+}/EGTA stimulation, respectively), (e) anti–activated-β2 integrin (mAb 24) alone upon Mg^{2+}/EGTA stimulation, and (f) activated-β2 integrin (mAb 24) and anti-CD47 antibody also upon Mg^{2+}/EGTA stimulation. Nucleus stained with DAPI.

Condition	τ_1 (ps)	a_1 (%)	τ_m (ps)
High-affinity β_2 integrin (donor only) + Mg^{2+}/EGTA	2905 ± 20	100 ± 0	2906 ± 20
High-affinity β_2 integrin + CD47 (B6H12) + Mg^{2+}/EGTA	956 ± 70[a]	28 ± 1	2392 ± 40[a]

Values represent means ± SEM for $n = 20$ for each condition.
[a]$p < 0.001$ vs. β_2 integrin donor only.

TABLE 3: FLIM analysis of high-affinity conformation of β_2 integrin–CD47 interactions.

blocked with 5% FBS in PBS at room temperature. A murine mAb to CD47 (B6H12) directly conjugated with Alexa 594 and a polyclonal Ab to β_2 integrins were diluted in PBS–5% FBS and incubated overnight at 4°C. As controls mAbs to PSGL-1 or αL integrin were used. Unlabeled primary Abs were detected using Alexa Fluor 488– or Alexa Fluor 594–conjugated secondary Abs when they corresponded. Protein interactions were defined by time-correlated single-photon counting FLIM as previously described (Mandal *et al.*, 2008; Bair *et al.*, 2012). The fluorescence baseline lifetime of Alexa Fluor 488 (donor fluorophore, αL or β_2 integrin) was calculated by single-exponential-decay fitting of fluorescence emission in the absence of Alexa Fluor 594 (acceptor fluorophore). For samples stained for both donor and acceptor, lifetimes were fitted to a biexponential decay with lifetime of one component fixed to the donor-only lifetime. The lifetime for the interacting component, τ_1, and the fractional contributions for the percentage of interacting fluorophores, a_1, were determined. Four or more separate experiments were performed, with n reported as total number of cells analyzed, and within each cell at least 10 different areas were used to determine the mean value. A Plan APO VC 60× oil DC N2 objective 1.4 NA, mounted on a Nikon Ti-E inverted microscope equipped with filter cubes used for DAPI, fluorescein isothiocyanate, and tetramethylrhodamine isothiocyanate fluorophores (Nikon), was used for epifluorescence and FLIM as described (Mandal *et al.*, 2008; Bair *et al.*, 2012). Nikon Elements 3.10 imaging software was used to collect epifluorescence data. For FLIM acquisition, Becker and Hickl (Berlin, Germany) a BDL-488-SMC Picosecond Diode Laser and both long-pass (HQ500LP) and bandpass (HQ435/50) emission filters were used in combination with a hybrid detector (HPM-100-40 GaAsP hybrid detector) integrated with a Hamamatsu (Hamamatsu, Japan) R10467-40 hybrid photomultiplier tube. Becker and Hickl SPCM software with detector controller card was used to acquire FLIM data, and SPCImage 3.0 (Becker and Hickl, Berlin, Germany) software was used for FLIM analysis.

Statistical analysis
Data are expressed as the mean ± SEM unless otherwise stated. Statistical analyses by Student's t test or by analysis of variance followed by the Newman–Keuls test were performed with Prism software (GraphPad, La Jolla, CA) and considered statistically significant at $p < 0.05$.

REFERENCES
Alcaide P, Maganto-Garcia E, Newton G, Travers R, Croce KJ, Bu Dx, Luscinskas FW, Lichtman AH (2012). Difference in Th1 and Th17 lymphocyte adhesion to endothelium. J Immunol 188, 1421–1430.

Andrew D, Shock A, Ball E, Ortlepp S, Bell J, Robinson M (1993). KIM185, a monoclonal antibody to CD18 which induces a change in the conformation of CD18 and promotes both LFA-1- and CR3-dependent adhesion. Eur J Immunol 23, 2217–2222.

Azcutia V, Stefanidakis M, Tsuboi N, Mayadas T, Croce KJ, Fukuda D, Aikawa M, Newton G, Luscinskas FW (2012). Endothelial CD47 promotes vascular endothelial-cadherin tyrosine phosphorylation and participates in T cell recruitment at sites of inflammation in vivo. J Immunol 189, 2553–2563.

Bair AM, Turman MV, Vaine CA, Panettieri RAJr, Soberman RJ (2012). The nuclear membrane leukotriene synthetic complex is a signal integrator and transducer. Mol Biol Cell 23, 4456–4464.

Barclay AN (2009). Signal regulatory protein alpha (SIRP[alpha])/CD47 interaction and function. Curr Opin Immunol 21, 47–52.

Brittain JE, Han J, Ataga KI, Orringer EP, Parise LV (2004). Mechanism of CD47-induced alpha4beta1 integrin activation and adhesion in sickle reticulocytes. J Biol Chem 279, 42393–42402.

Brown EJ, Frazier WA (2001). Integrin-associated protein (CD47) and its ligands. Trends Cell Biol 11, 130–135.

Brown E, Hooper L, Ho T, Gresham H (1990). Integrin-associated protein: a 50-kD plasma membrane antigen physically and functionally associated with integrins. J Cell Biol 111, 2785–2794.

Chen C, Mobley JL, Dwir O, Shimron F, Grabovsky V, Lobb RR, Shimizu Y, Alon R (1999). High affinity very late antigen-4 subsets expressed on T cells are mandatory for spontaneous adhesion strengthening but not for rolling on VCAM-1 in shear flow. J Immunol 162, 1084–1095.

Constantin G, Majeed M, Giagulli C, Piccio L, Kim JY, Butcher EC, Laudanna C (2000). Chemokines trigger immediate beta2 integrin affinity and mobility changes: differential regulation and roles in lymphocyte arrest under flow. Immunity 13, 759–769.

Cooper D, Lindberg FP, Gamble JR, Brown EJ, Vadas MA (1995). Transendothelial migration of neutrophils involves integrin-associated protein (CD47). Proc Natl Acad Sci USA 92, 3978–3982.

de Vries HE, Hendriks JJA, Honing H, de Lavalette CR, van der Pol SMA, Hooijberg E, Dijkstra CD, van den Berg TK (2002). Signal-regulatory protein alpha-CD47 interactions are required for the transmigration of monocytes across cerebral endothelium. J Immunol 168, 5832–5839.

Dransfield I, Hogg N (1989). Regulated expression of Mg2+ binding epitope on leukocyte integrin alpha subunits. EMBO J 8, 3759–3765.

Fortin G, Raymond M, Van VQ, Rubio M, Gautier P, Sarfati M, Franchimont D (2009). A role for CD47 in the development of experimental colitis mediated by SIRPa+CD103- dendritic cells. J Exp Med 206, 1995–2011.

Han MH et al. (2012). Janus-like opposing roles of CD47 in autoimmune brain inflammation in humans and mice. J Exp Med 209, 1325–1334.

Hogg N, Patzak I, Willenbrock F (2011). The insider's guide to leukocyte integrin signalling and function. Nat Rev Immunol 11, 416–426.

Isenberg JS, Roberts DD, Frazier WA (2008). CD47: a new target in cardiovascular therapy. Arterioscler Thromb Vasc Biol 28, 615–621.

Kim M, Carman CV, Yang W, Salas A, Springer TA (2004). The primacy of affinity over clustering in regulation of adhesiveness of the integrin αLβ2. J Cell Biol 167, 1241–1253.

Lefort CT, Rossaint J, Moser M, Petrich BG, Zarbock A, Monkley SJ, Critchley DR, Ginsberg MH, Fässler R, Ley K (2012). Distinct roles for talin-1 and kindlin-3 in LFA-1 extension and affinity regulation. Blood 119, 4275–4282.

Ley K, Bullard DC, Arbones ML, Bosse R, Vestweber D, Tedder TF, Beaudet AL (1995). Sequential contribution of L- and P-selectin to leukocyte rolling in vivo. J Exp Med 181, 669–675.

Lim YC, Wakelin MW, Henault L, Goetz DJ, Yednock T, Cabanas C, Sanchez-Madrid F, Lichtman AH, Luscinskas FW (2000). Alpha4beta1-integrin activation is necessary for high-efficiency T-cell subset interactions with VCAM-1 under flow. Microcirculation 7, 201–214.

Lindberg FP, Bullard DC, Caver TE, Gresham HD, Beaudet AL, Brown EJ (1996). Decreased resistance to bacterial infection and granulocyte defects in IAP-deficient mice. Science 274, 795–798.

Luque A, Gomez M, Puzon W, Takada Y, Sanchez-Madrid F, Cabanas C (1996). Activated conformations of very late activation integrins detected by a group of antibodies (HUTS) specific for a novel regulatory region (355–425) of the common b1 chain. J Biol Chem 271, 11067–11075.

Mandal AK *et al.* (2008). The nuclear membrane organization of leukotriene synthesis. Proc Natl Acad Sci USA 105, 20434–20439.

McDonald JF, Zheleznyak A, Frazier WA (2004). Cholesterol-independent interactions with CD47 enhance alpha v beta3 avidity. J Biol Chem 279, 17301–17311.

Miller LJ, Schwarting R, Springer TA (1986). Regulated expression of the Mac-1, LFA-1, p150,95 glycoprotein family during leukocyte differentiation. J Immunol 137, 2891–2900.

Parkos CA, Colgan SP, Liang TW, Nusrat A, Bacarra AE, Carnes DK, Madara JL (1996). CD47 Mediates post-adhesive events required for neutrophil migration across polarized intestinal epithelia. J Cell Biol 132, 437–450.

Quinn MT, Swain SD, Parkos CA, Jutila KL, Siemsen DW, Kurk SL, Jesaitis AJ, Jutila MA (2001). A carbohydrate neoepitope that is up-regulated on human mononuclear leucocytes by neuraminidase treatment or by cellular activation. Immunology 104, 185–197.

Salas A, Shimaoka M, Kogan AN, Harwood C, von Andrian UH, Springer TA (2004). Rolling adhesion through an extended conformation of integrin aLb2 and relation to a I and a I-like domain interaction. Immunity 20, 393–406.

Shamri R, Grabovsky V, Gauguet JM, Feigelson S, Manevich E, Kolanus W, Robinson MK, Staunton DE, von Andrian UH, Alon R (2005). Lymphocyte arrest requires instantaneous induction of an extended LFA-1 conformation mediated by endothelium-bound chemokines. Nat Immunol 6, 497–506.

Shimaoka M, Takagi J, Springer TA (2002). Conformational regulation of integrin structure and function. Annu Rev Biophys Biomol Struct 31, 485–516.

Sircar M *et al.* (2007). Neutrophil transmigration under shear flow conditions in vitro is junctional adhesion molecule-C independent. J Immunol 178, 5879–5887.

Smith A, Carrasco YR, Stanley P, Kieffer N, Batista FD, Hogg N (2005). A talin-dependent LFA-1 focal zone is formed by rapidly migrating T lymphocytes. J Cell Biol 170, 141–151.

Snapp KR, Wagers AJ, Craig R, Stoolman LM, Kansas GS (1997). P-selectin glycoprotein ligand-1 is essential for adhesion to P- selectin but not E-selectin in stably transfected hematopoietic cell lines. Blood 89, 896–901.

Stefanidakis M, Newton G, Lee WY, Parkos CA, Luscinskas FW (2008). Endothelial CD47 interaction with SIRPg is required for human T-cell transendothelial migration under shear flow conditions in vitro. Blood 112, 1280–1289.

Su X, Johansen M, Looney MR, Brown EJ, Matthay MA (2008). CD47 deficiency protects mice from lipopolysaccharide-induced acute lung injury and *Escherichia coli* pneumonia. J Immunol 180, 6947–6953.

Ticchioni M, Raimondi V, Lamy L, Wijdenes J, Lindberg FP, Brown EJ, Bernard A (2001). Integrin-associated protein (CD47/IAP) contributes to T cell arrest on inflammatory vascular endothelium under flow. FASEB J 15, 341–350.

Yang J, Hirata T, Croce K, Merrill-Skoloff G, Tchernychev B, Williams E, Flaumenhaft R, Furie BC, Furie B (1999). Targeted gene disruption demonstrates that P-selectin glycoprotein ligand 1 (PSGL-1) is required for P-selectin-mediated but not E-selectin-mediated neutrophil rolling and migration. J Exp Med 190, 1769–1782.